



# Dynamic Contrast-Enhanced Breast MRI Findings Predictive of Malignancy in MRI-Only Breast Lesions Examined by MR-Guided Biopsy: A Single-Center Experience

*MRG'de Saptanabilen ve MR Eşliğinde Biyopsi Yapılan Meme Lezyonlarında Maligniteyi Öngören Dinamik Kontrastlı Meme MRG Bulguları: Tek Merkez Deneyimi*

Almila Coskun Bilge<sup>1</sup>, Hale Aydın<sup>2</sup>, Isil Esen Bostancı<sup>1</sup>

<sup>1</sup>Department of Radiology, Dr. Abdurrahman Yurtaslan Ankara Oncology Training and Research Hospital, Ankara;

<sup>2</sup>Department of Radiology, University of Health Sciences, Gulhane Faculty of Medicine, Ankara

## ABSTRACT

**Aim:** It was aimed to investigate the association between dynamic contrast-enhanced magnetic resonance imaging (MRI) findings and malignancy in suspicious MRI-only breast lesions performed by MR-guided biopsy.

**Material and Method:** Between December 2014 and December 2020, 57 suspicious MRI-only lesions were identified. Among these, 46 lesions underwent MR-guided wire localization and excisional biopsy, while 11 underwent MR-guided core biopsy. Clinical data, MRI findings, biopsy results, and information about the MR-guided biopsy procedures were collected. The predictive value of MRI findings in determining malignancy was analyzed.

**Results:** According to biopsy results, 14 (24.6%) of the 57 lesions were malignant, and 43 (75.4%) were benign. The malignancy rate was significantly higher in lesions in the lower inner quadrant (55.5%,  $p=0.040$ ) and those with a washout kinetic curve than those with persistent and plateau curves ( $p=0.034$ ). Malignancy was detected in 83.3% of the lesions classified as BI-RADS-MRI category 5 versus only 17.6% of those classified as BI-RADS-MRI category 4 ( $p=0.006$ ).

**Conclusion:** Kinetic curve type and BI-RADS-MRI category were identified as MRI findings predicting the malignancy of lesions assessed by MR-guided biopsy. According to MR-guided biopsy, BI-RADS-MRI category 5 lesions and those with washout kinetic curves were significantly more likely to be malignant.

**Key words:** image-guided biopsy; magnetic resonance imaging; breast cancer; breast imaging reporting and data system

## ÖZET

**Amaç:** MR kılavuzluğunda biyopsi yapılan, yalnızca MRG'de izlenebilen şüpheli meme lezyonlarının dinamik kontrastlı manyetik rezonans görüntüleme (MRG) bulguları ile malignite arasındaki ilişkiyi araştırmak amaçlandı.

**Materyal ve Metot:** Aralık 2014 ile Aralık 2020 tarihleri arasında yalnızca MRG'de izlenebilen 57 şüpheli meme lezyonu tespit edildi; bunların 46'sına MR kılavuzluğunda tel lokalizasyonu ve eksizyonel biyopsi, 11'ine MR kılavuzluğunda kor biyopsi uygulandı. Hastaların klinik verileri, MR bulguları, biyopsi sonuçları ve MR eşliğinde biyopsi işlemlerine ilişkin veriler kaydedildi. Lezyonun MR bulgularının, malignite açısından öngörü değeri analiz edildi.

**Bulgular:** Biyopsi sonuçlarına göre 57 lezyonun 14'ü (%24,6) malign, 43'ü (%75,4) benign idi. Alt iç kadranda yerleşen lezyonlarda (%55,5,  $p=0,040$ ) ve wash-out kinetik eğrisi olanlarda, persistan ve plato eğriye sahip olanlara göre ( $p=0,034$ ) malignite oranı anlamlı olarak daha yüksekti. BI-RADS-MRI kategori 5 olarak sınıflandırılan lezyonların %83,3'ünde malignite tespit edilirken, BI-RADS-MRI kategori 4 olarak sınıflandırılan lezyonların sadece %17,6'sında malignite tespit edildi ( $p=0,006$ ).

**Sonuç:** Kinetik eğri tipi ve BI-RADS-MRI kategorisi, MR eşliğinde biyopsi ile değerlendirilen lezyonların malignitesini öngören MR bulguları olarak belirlendi. BI-RADS-MRI kategori 5 lezyonlar ve wash-out kinetik eğrisi olan lezyonların MR kılavuzluğunda yapılan biyopsi sonrası elde edilen patoloji sonucunda malign raporlanma olasılıkları anlamlı derecede yüksekti.

**Anahtar kelimeler:** görüntü kılavuzluğunda biyopsi; manyetik rezonans görüntüleme; meme kanseri; meme görüntüleme raporlama ve veri sistemi

**İletişim/Contact:** Almila Coşkun Bilge, Dr. Abdurrahman Yurtaslan Ankara Oncology Training and Research Hospital, Mehmet Akif Ersoy Mah 13. Cadde No: 56 Post code:06200 Yenimahalle Ankara • Tel: +90 312 336 0909 – 4654 • E-mail: almilacoskun@gmail.com • Geliş/Received: 01.09.2023 • Kabul/Accepted: 04.11.2023

**ORCID:** Almila Coşkun Bilge, 0000-0002-0371-4194 • Hale Aydın, 0000-0002-4789-4641 • Isil Esen Bostancı, 0000-0001-6026-0830

## Introduction

Dynamic contrast-enhanced MRI is widely used in the evaluation of breast lesions<sup>1,2</sup>. Magnetic resonance imaging is more sensitive than mammography (MG) or ultrasound (US) in detecting breast lesions<sup>3,4</sup>. The sensitivity of MRI for breast cancer can reach up to 100%<sup>5,6</sup>. As a result of this high sensitivity, MRI can reveal lesions that are occult on MG and US, which are termed MRI-only lesions<sup>3</sup>. The American Cancer Society (ACR) and European Society of Breast Imaging (EUSOBI) guidelines recommend MR-guided tissue sampling for MRI-only lesions suspected of being malignant according to evaluation with the Breast Imaging Reporting and Data Analysis (BI-RADS) MRI lexicon<sup>4,7</sup>. Tissue sampling of these lesions uses MR-guided wire localization (MGWL) followed by excisional biopsy or MR-guided core biopsy (MGCB). MR-guided wire localization is relatively easy to perform and yields good results in complete excision because it is followed by excisional biopsy. However, the surgery performed after wire localization is invasive, costly, and carries the risk of perioperative complications<sup>4,8</sup>. Percutaneous MGCB is a safe, less invasive, faster, and cheaper procedure that reduces open biopsies in benign lesions<sup>4,8</sup>. Unfortunately, this method is challenging with small lesions and those in specific locations (superficial, medial, in the anterior retroareolar region, or near the chest wall)<sup>9,10</sup>. Additionally, many centers in Türkiye do not perform MR-guided interventional methods because they lack the technological or logistical capacity or experience to perform the procedures.

Normal breast parenchyma and many benign lesions can mimic malignancy in terms of morphological and contrast enhancement features on MRI, thereby reducing the specificity of breast MRI<sup>11</sup>. This situation may result in unnecessary MR-guided biopsies, which is a time-consuming and expensive procedure. Improving the differentiation of benign and malignant lesions in pre-biopsy MRI images is vital in determining the need for biopsy and evaluating the concordance of pathological and radiological findings<sup>12</sup>.

In this study, we aimed to present our clinical experience with MGWL and MGCB procedures performed in our center and to investigate the predictive value of initial MRI findings in detecting malignancy in suspicious MRI-only lesions sampled by MGWL and MGCB.

## Material and Methods

Our institute's Scientific Research Ethics Committee approved this retrospective study (2022–08/130), and the participating patients provided written informed consent.

### Patients

We retrospectively reviewed the data of 64 breast lesions in 62 women who underwent MGWL and excisional biopsy or MGCB in our center between December 2014 and December 2020. Three women were lost to follow-up before undergoing the recommended biopsy procedure. Four lesions in two women were excluded from the study because a core biopsy couldn't be conducted due to their inability to be visualized on MRI during the procedure. (Fig. 1). As a result, 46 women who underwent MGWL (age range: 27–75 years, mean age: 52 years) and 11 women who underwent MGCB (age range: 19–67 years, mean age: 47 years) were included in the study. The mean age of the study group was 49 years (range: 19–75 years).

### Data Collection

Medical records in the hospital electronic data archive were reviewed for patient age, physical examination findings, family history of breast cancer, MRI indication, radiology and pathology reports, and clinical follow-up results. Pre-biopsy MRI images were retrieved from the electronic data archive of the radiology department and reviewed together with MG or US findings. The type of biopsy performed and post-biopsy complications were determined from the patients' medical records. Procedure time was calculated as the difference between the timestamp of the last MR image acquired after wire or clip localization and the first localizer MR image in the electronic archive.

### Magnetic Resonance Imaging Technique

Magnetic resonance imaging images were acquired with patients in the prone position using a dedicated 1.5-Tesla (T) MR scanner (SignaHDx; GE Healthcare, Wisconsin, USA) and breast array coil. Imaging parameters consisted of axial T1-weighted (T1W) images (repetition time/echo time [TR/TE]: 400/8.8, field of view (FOV): 320 mm, matrix: 448×224, number of excitations (NEX): 1, and slice thickness (ST): 5 mm); axial short tau inversion recovery (STIR) (TR/TE: 6500/45, inversion time [TI]: 150 ms, FOV: 320 mm, matrix: 416×224, NEX: 1, and ST: 5 mm); dynamic

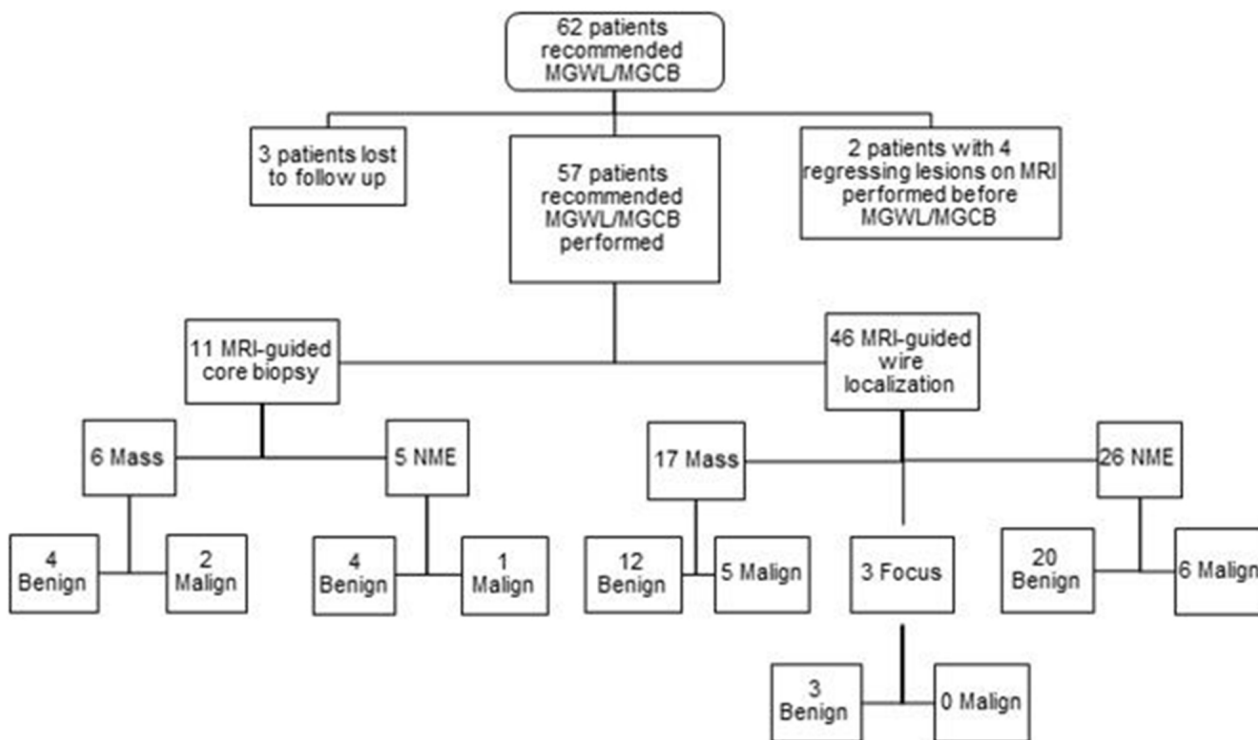


**Figure 1.** Inclusion flowchart. MGWL, MR-guided wire localization; MGCB, MR-guided core biopsy; NME, non-mass enhancement.

axial fat-saturated (FS) T1W images (before and after contrast injection) (TR/TE: 4/1.5, flip angle: 10°, FOV: 320 mm, matrix: 350×350, NEX: 1, and ST: 2.8 mm). An intravenous injection of 0.1 mmol/kg gadobutrol/gadopentetate dimeglumine was administered as a contrast material, followed by a saline bolus. Pre-contrast images were obtained once, and post-contrast images were obtained five times at intervals of 80 seconds. Standard subtraction images, maximum-intensity projection (MIP), and multiplanar reconstruction (MPR) were rendered automatically on a workstation. Kinetic curves of the lesions were constructed automatically by the device using a time-intensity curve.

### Magnetic Resonance Imaging Findings

In our center, dynamic contrast-enhanced breast MRI was performed on all patients before MGWL or MGCB. Magnetic resonance imaging images were interpreted retrospectively on one workstation by three radiologists experienced in breast imaging. The radiologists were informed about the clinical course of the patients and their MG and US imaging findings. Each case was evaluated through a consensus between these three radiologists by interpreting the imaging findings according to the BI-RADS-MRI descriptors

(American College of Radiology, 2013). All lesions were classified as BI-RADS category 4 or 5 based on MRI findings.

The location of the target lesions in the breast was determined by examining dynamic breast MRI images and categorized as central, upper inner, upper outer, lower inner, and lower outer quadrant. Breast density (BD) and background parenchymal enhancement (BPE) were categorized according to the BI-RADS lexicon<sup>13</sup>. Breast density was classified as predominantly fatty, scattered, heterogeneously dense, or extremely dense based on the ratio of fibroglandular tissue in the breast on T1W images. Background parenchymal enhancement was determined by assessment of the intensity of fibroglandular tissue contrast enhancement in the early phase of post-contrast T1W FS sequence and was interpreted as minimal, mild, moderate, and marked<sup>13</sup>. The largest lesion dimension was measured from post-contrast T1W FS, MIP, and MPR images.

Morphology of the lesions was classified as mass, non-mass enhancement (NME), and focus as defined in the BI-RADS lexicon. The shape of the mass/focus (circumscribed or irregular), distribution of NME (linear, segmental, focal, and regional), and internal enhancement pattern of each lesion (homogeneous and heterogeneous,

as well as ring pattern for masses and foci) were analyzed on post-contrast subtraction, MIP, and sagittal MPR images<sup>13,14</sup>. The kinetic enhancement pattern of the lesions was characterized as washout, plateau, or persistent according to the kinetic curves obtained.

#### *Indications for MR-Guided Wire Localization or MR-Guided Core Biopsy*

MR-guided wire localization or MGCB was performed on a single lesion in each patient. Fifty-seven suspicious lesions were detected only on MRI and were occult on MG and US. Therefore, MGWL and excisional biopsy or MGCB were recommended for the pathological diagnosis of BI-RADS-MRI 4 and 5 lesions. MR-guided wire localization was preferred in 30 lesions with difficult locations for MGCB (anterior or subareolar, far posterior, or superficial [ $<2$  cm from the skin]), eight lesions scheduled for surgical excision, and eight patients with small breasts. MR-guided core biopsy was performed for the remaining lesions ( $n=11$ ).

#### *MR-Guided Biopsy Procedures*

All MR-guided biopsies were performed in a 1.5-T MR scanner (SignaHDx; GE Healthcare, Wisconsin, USA) with the patient in the prone position, using a breast array coil and grid-localization system. During interventional procedures for lesions in the inner quadrants, a cardboard barrier was used to prevent the contralateral breast from entering the coil for a medial approach. In the lateral approach, both breasts were in the coil. The grid plate was placed over the breast in the target lesion area according to the diagnostic MR image, and compression sufficient to stabilize the breast was applied. A pre-contrast image was obtained to confirm the breast was positioned with the target lesion within the area of accessibility. By examining the images, the estimated location of the lesion was marked externally by placing cotton soaked with gadolinium contrast agent on the skin. Gadobutrol/gadopentetate dimeglumine at a 0.1 mmol/kg dose was intravenously injected as a contrast agent and then flushed with saline. The lesion's exact location was confirmed and positioned according to the marker by evaluating post-contrast images. The distance of the lesion from the skin was noted. The skin entry site was prepared by cleaning with an antiseptic solution and anesthetizing with 1% lidocaine.

#### *MR-Guided Wire Localization Technique*

An MR-compatible 18-gauge needle and hook wire were inserted into the desired depth through the

prepared skin entry site. Considering the calculated skin-lesion distance, the needle tip was inserted up to 1 cm beyond the target lesion. Sagittal and axial contrast-enhanced images were obtained to confirm the appropriate needle location. The needle appeared as a hypointense structure in these images because of the susceptibility artifact (Fig. 2). The wire was deployed when the needle was in the desired location. Contrast-enhanced T1W images and two-view MG were performed to document wire location.

#### *MR-Guided Core Biopsy Technique*

An MR-compatible 14-gauge coaxial system consisting of a needle and sheath was inserted through the skin to the calculated depth for the tip of the needle to reach the lesion margin. Axial sequence images were acquired to confirm the correct positioning of the system (Fig. 3). The needle was then removed, and a 14-gauge MRI-compatible automatic core biopsy needle was inserted through the sheath.

A minimum of five specimens were obtained from the lesion. After sampling, an MRI-safe marker clip was placed at the biopsy site via the sheath. The coaxial system was then removed. Compression was applied manually to the skin entry and needle sampling sites to achieve hemostasis. After the procedure, a two-view MG was performed to verify the clip location.

#### *Pathological Data Evaluation*

The pathology results of the biopsied lesions were obtained from our center's electronic data archive. The results were classified as benign or malignant and recorded. The radiologists evaluated the concordance between pathology and radiology using dynamic contrast-enhanced MRI findings.

#### *Statistical Analysis*

Statistical analyses were performed using the IBM Statistical Package for Social Sciences (SPSS) package program version 20.0 (IBM Corporation, Armonk, NY, USA). Data were grouped according to benign and malignant lesions. Categorical data such as family history, MRI indication, MR-guided biopsy procedure, pathological diagnosis, and distribution of MRI findings were expressed as numbers and percentages. Continuous variables, including patient age and lesion size, were expressed as mean  $\pm$  standard deviation (minimum-maximum values) or median (25–75% percentiles). Normality analyses of continuous

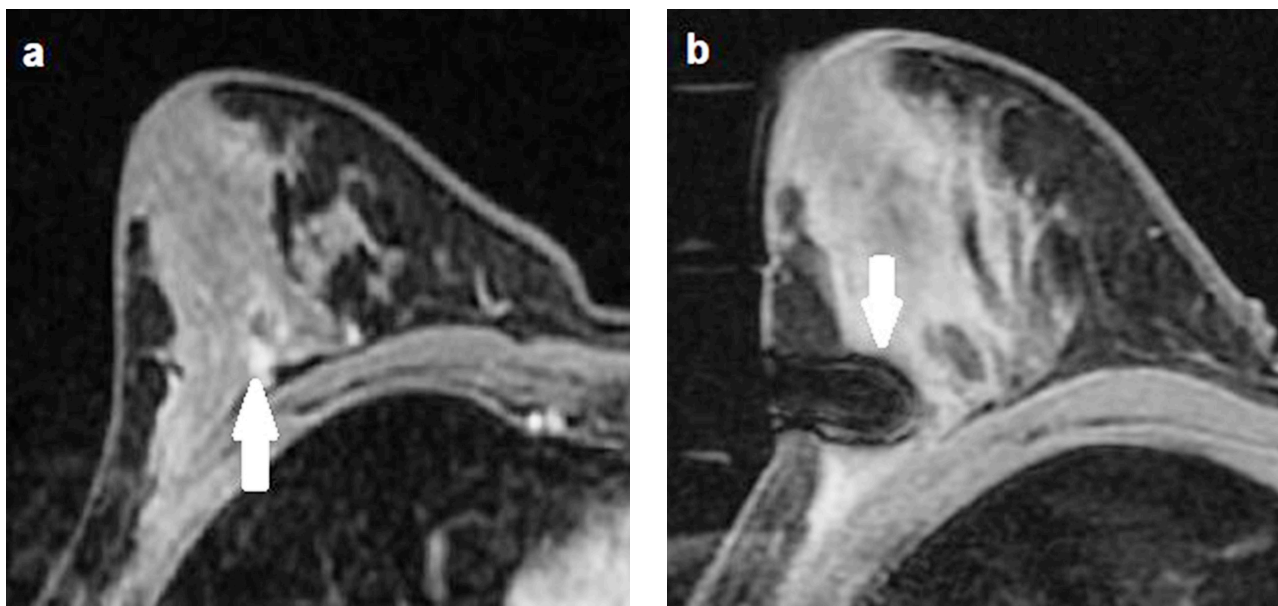


**Figure 2.** a–b. A 34-year-old woman with known breast cancer in the right breast undergoing imaging to investigate the extent of disease. Axial post-contrast T1-weighted fat-suppressed MR shows a focus suspicious for malignancy located near the chest wall in right breast (arrow)(a). Low signal intensity due to susceptibility artifact of the needle is seen in axial post-contrast T1-weighted fat-suppressed MR image obtained during MR-guided wire localization (arrow). The final pathological diagnosis was sclerosing adenosis (b).

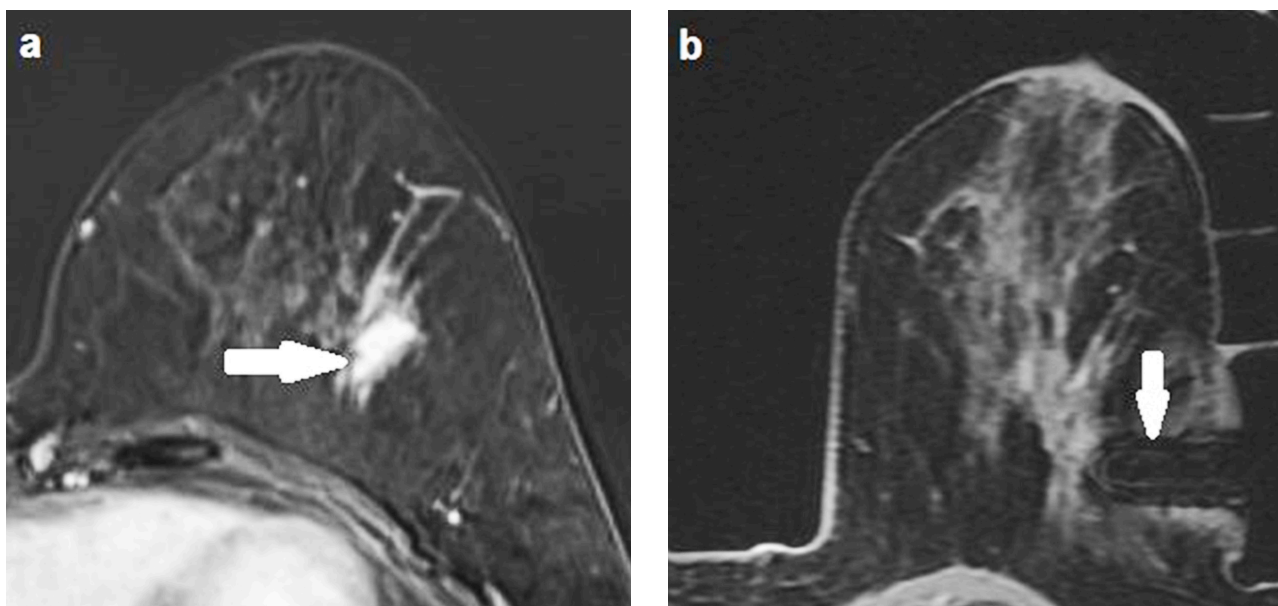


**Figure 3.** a–b. A 49-year-old woman with equivocal sonographic findings in right breast. Axial post-contrast T1-weighted fat-suppressed MR subtraction image shows mass lesion with microlobulated margin and heterogeneous internal enhancement pattern in the left breast (arrow)(a). Low signal intensity due to susceptibility artifact of the coaxial system is seen in axial post-contrast T1-weighted fat-suppressed MR image obtained during MR-guided core biopsy (arrow) (b).

variables were performed using the Shapiro-Wilk test. In the statistical analysis between groups, the independent samples t-test was used for continuous variables if normally distributed, and the Mann-Whitney U test was used if non-normally distributed. Logistic regression analysis was performed using the categorical variables, including family history, MR indication

category, MR-guided biopsy procedure, lesion location, BD, BPE, lesion morphology, lesion shape or distribution, lesion enhancement pattern, lesion kinetic curve type, and BI-RADS-MRI category to assess their association with malignancy. A p-value less than 0.05 was considered statistically significant.

**Results**

*Lesion Histologic Results*

Biopsy results indicated that 14 of 57 lesions (24.6%) were malignant and 43 (75.4%) were benign. The pathologic diagnoses obtained are shown in Table 1. The majority of malignant lesions (57.1%) had a pathological diagnosis of ductal carcinoma in situ (DCIS). The most frequently diagnosed benign lesion (18.6%) was sclerosing adenosis.

*Breast MRI Indications*

Indications for breast MRI included imaging for problem-solving (34/57, 59.6%), evaluation of disease extent in patients with known breast cancer (12/57, 21.1%), and screening of women at high/moderate risk (11/57, 19.3%). Of the high/moderate-risk women, 5 had a family history of breast cancer, 3 had a personal history of breast cancer, and 3 had a previously diagnosed lesion with atypia. Magnetic resonance imaging for the indication of problem-solving was performed in patients with equivocal MG or US findings (n=24), nipple discharge (n=9), or primary carcinoma of unknown origin with bone metastases (n=1).

The malignancy rate was higher in the group that underwent MRI for the investigation of breast cancer extent (41.7%) than for the indications of problem-solving (23.5%) and screening (9.1%). However, the groups had no statistically significant difference (p=0.222).

Malignancy was detected in 21.4% of the patients with positive family history and 25.6% of those without (p=0.754) (Table 2).

*Magnetic Resonance Imaging Findings and Lesion Morphologic Features*

Dynamic contrast-enhanced MRI findings were evaluated to determine the predictors of malignancy in patients undergoing MR-guided biopsy. The mean size of the benign lesions was 14 mm (range, 4–50 mm), whereas it was 18 (range, 4–50) mm in the malignant lesions, which was not a statistically significant difference (p=0.590).

According to the location of the lesions in the breast, malignancy rates were 55.5%, 28.6%, 21.4%, and 17.4% in the lower inner quadrant, central region, lower outer quadrant, and upper outer quadrants, respectively. Pathology results indicated all upper-inner quadrant lesions were benign. The lower inner quadrant location was significantly associated with malignancy

**Table 1.** The pathologic diagnoses of the lesions

Pathology	No. of lesions n (percentage)	Pathology	No. of lesions n (percentage)
Malignant lesions	14 (24.6%)	Benign lesions	43 (75.4%)
DCIS	8 (14%)	Sclerosing adenosis	8 (14%)
IDC	5 (8.8%)	Fibroadenoma	7 (12.3%)
ILC	1 (1.8%)	Columnar cell hyperplasia	6 (10.5%)
		IDP	5 (8.8%)
		Fat necrosis	4 (7%)
		Fibrocystic changes	4 (7%)
		Hyalinized breast tissue	3 (5.3%)
		Epithelial hyperplasia	2 (3.5%)
		Adenosis	2 (3.5%)
		Lymph node	2 (3.5%)

DCIS: ductal carcinoma in-situ; IDC: invasive ductal carcinoma; ILC: invasive lobular carcinoma; IDP: intraductal papilloma.

**Table 2.** Comparison of benign and malignant lesions in terms of patients' age, lesion size, family history for breast cancer of patients, indications of breast MR and biopsy procedure

	Benign (n=43)	Malignant (n=14)	p-value	Odds ratio (95% CI)
<b>Age (year) (mean±SD)</b>	48.95±12.76	47.86±15.06	0.791	0.95 (0.42-2.02)
<b>Lesion median size (mm) (25%-75% percentiles)</b>	14 (9.00-20.00)	18 (9.75-20.50)	0.590	1.31 (0.87-2.50)
<b>Family history, n (percentage)</b>				
None	32 (56.1%)	11 (19.3%)	0.754	1.00
Positive	11 (19.3%)	3 (5.3%)		0.79 (0.18-3.37)
<b>MRI indications, n (%)</b>				
Breast cancer extent	7 (12.3%)	5 (8.8%)	0.222	1.00
Problem solving	26 (45.6%)	8 (14%)	0.237	0.43 (0.10-1.73)
High risk screening	10 (17.5%)	1 (1.8%)	0.102	0.14 (0.01-1.47)
<b>Procedure, n (%)</b>				
MR-guided core biopsy	8 (14%)	3 (5.3%)	0.147	1.00
MR-guided wire localization	35 (61.4%)	11 (19.3%)		0.37 (0.18-3.71)

CI: confidence interval; SD: standard deviation.

(p=0.040), with 6-fold higher odds of detecting malignancy than the upper outer quadrant.

When evaluated according to BD, malignancy rates were 33.3% in predominantly fatty, 10% in scattered, 31.2% in heterogeneously dense, and 11.1% in highly dense lesions. Although the malignancy rate was highest for lesions in predominantly fatty breasts, the difference was not statistically significant (p=0.431).

**Table 3.** The distribution of MRI findings of the lesions according to MR-directed US non-correlated and correlate

MRI findings	Benign, n (percentage)	Malignant, n (percentage)	p-value	Odds ratio (95% CI)
<b>Location</b>				
UOQ	19 (33.3%)	4 (7%)	0.335	1.00
UIQ	4 (7%)	0 (0%)	0.999	0.00
Central	5 (8.8%)	2 (3.5%)	0.522	1.90 (0.26–13.52)
LOQ	11 (19.3%)	3 (5.3%)	0.761	1.29 (0.24–6.88)
LIQ	4 (7%)	5 (8.8%)	0.040	5.93 (1.08–32.51)
<b>Breast density</b>				
Predominantly fatty	4 (7%)	2 (3.5%)	0.431	1.00
Scattered	9 (15.8%)	1 (1.8%)	0.270	0.22 (0.01–3.22)
Heterogeneously dense	22 (38.6%)	10 (17.5%)	0.920	0.90 (0.14–5.80)
Extremely dense	8 (14%)	1 (1.8%)	0.311	0.25 (0.01–3.66)
<b>BPE</b>				
Minimal	11 (19.3%)	4 (7%)	0.783	1.00
Mild	11 (19.3%)	6 (10.5%)	0.600	1.50 (0.32–6.83)
Moderate	16 (28.1%)	4 (7%)	0.643	0.68 (0.14–3.35)
Marked	5 (8.8%)	0 (0%)	0.999	0.00
<b>Morphology</b>				
Mass	16 (28%)	7 (12.3%)	0.810	1.00
NME	24 (42.1%)	7 (12.3%)	0.516	0.66 (0.19–2.26)
Focus	3 (5.3%)	0 (0%)	0.999	0.00
<b>Mass/Focus (n=26)</b>				
<i>Shape</i>				
Circumscribed	10 (17.5%)	3 (5.3%)	0.659	1.00
Irregular	9 (15.8%)	4 (7%)		1.48 (0.25–8.49)
<i>Enhancement</i>				
Homogeneous	10 (17.5%)	4 (7%)	0.997	1.00
Heterogeneous	8 (14%)	3 (5.3%)	0.943	0.93 (0.16–5.46)
Ring enhancement	1 (1.8%)	0 (0%)	1.000	0.00
<b>NME</b>				
<i>Distribution</i>				
Linear	8 (14%)	3 (5.3%)	0.985	1.00
Segmental	2 (3.5%)	1 (1.8%)	0.837	1.33 (0.86–20.70)
Focal	10 (17.5%)	3 (5.3%)	0.813	0.80 (0.12–5.09)
Regional	4 (7%)	0 (0%)	0.999	0.00
<i>Enhancement</i>				
Homogeneous	8 (14%)	14 (24.6%)	0.813	1.00
Heterogeneous	4 (7%)	5 (8.8%)		1.25 (0.19–7.92)
<b>Kinetic curve type</b>				
Persistent	10 (17.5%)	1 (1.8%)	0.004	1.00
Plateau	22 (38.6%)	1 (1.8%)	0.590	0.45 (0.02–8.02)
Washout	11 (19.3%)	12 (21%)	0.034	10.90 (1.19–99.68)
<b>BI-RADS-MRI</b>				
Category 4	42 (73.6%)	9 (15.8%)	0.006	1.00
Category 5	1 (1.8%)	5 (8.8%)		23.33 (2.42–224.61)

CI: confidence interval; UOQ: upper outer quadrant; UIQ: upper inner quadrant; LOQ: lower outer quadrant; LIQ: lower inner quadrant; BPE: background parenchymal enhancement; NME: non-mass enhancement.

Considering BPE, the malignancy rate was 26.7% in breasts with minimal BPE, 35.3% with mild BPE, and 20% with moderate BPE. All lesions in breasts with marked parenchymal enhancement were benign (Table 3).

Regarding lesion morphology, all three lesions assessed as focus lesions had benign pathology results. Although the malignancy rate was higher in mass lesions (30.4%) than in those with NME (22.6%), it was not statistically significant ( $p=0.810$ ). In addition,

no meaningful relationship was found between the shape of mass and focused lesions and malignancy ( $p=0.659$ ). Mass and focus lesions with homogeneous (28.6%) and heterogeneous (27.3%) enhancement had similar malignancy rates. Only one ring-enhanced mass lesion was diagnosed as benign. When the distribution of NME lesions on MRI was evaluated as linear, segmental, focal, and regional, the malignancy rates in these subgroups were 27.3%, 33.3%, 23.1%, and 0%, respectively. Malignancy was detected more in lesions with segmental distribution than those with linear and focal distribution. Still, it was not statistically significant ( $p=0.837$ ). Furthermore, no statistically significant correlation was found between the rate of malignancy and the enhancement patterns of NME lesions ( $p=0.813$ ).

When the distribution of malignant lesions according to the kinetic curve of all lesions was examined, the highest rate (52.2%) was found in lesions with a washout kinetic curve ( $p=0.034$ ). Lesions with persistent and plateau kinetic curves had significantly lower rates of malignancy (9.1% and 4.3%, respectively;  $p=0.004$ ).

#### *BI-RADS Category*

The malignancy rates detected in BI-RADS category 4 and 5 lesions were 17.6% and 83.3%, respectively ( $p=0.006$ ). The odds of malignancy were 21 times higher for BI-RADS category 5 lesions than BI-RADS category 4 lesions.

#### *MR-guided Biopsy Procedures*

MR-guided core biopsy was performed in 11 of the 57 patients (19.3%), and MGWL was conducted in the other 46 patients (80.7%). When compared according to the type of biopsy procedure performed, no statistically significant difference was found in the detected malignancy rates ( $p=0.147$ ).

#### *Follow-up*

There was radiologic-pathologic concordance in all lesions. A follow-up MRI was recommended six months later in cases with benign pathological diagnoses. Follow-up MRI was obtained from 43 patients 6, 12, and 24 months after biopsy. None of these patients exhibited findings suggestive of malignancy and were assessed as BI-RADS category 2 or 3.

## **Discussion**

Breast MRI can detect lesions not seen on US and MG in 10–39% of examined patients<sup>15</sup>. MR-guided wire localization and MGCB biopsy are appropriate, safe, and accurate methods in the pathological diagnosis of clinically and mammographically occult breast lesions<sup>9</sup>.

Unlike previous studies in the literature, we included patients who underwent MGWL and those who experienced MGCB in the present study. Instead of comparing procedures, we focused on evaluating the ability of MRI findings to predict the malignancy of lesions for which technically challenging MR-guided biopsy procedures are recommended for tissue diagnosis. Of the 61 lesions initially planned for MGCB, the procedure could not be performed in 4 cases (6.5%, all with NME) because the lesions could not be visualized. This finding is consistent with the literature<sup>1,5,10</sup>. Positioning, compression, or the phase of the patient's menstrual cycle are possible reasons why the lesion was not visible on images obtained on the day of the procedure<sup>10</sup>. Gao et al. found this rate to be 2%, which they attributed to the high rate of newly diagnosed breast cancer patients (62%) in their study<sup>9</sup>.

Complications such as significant bleeding, infection, vasovagal reaction, contralateral skin puncture, and wire dislocation were not observed during or after any of the procedures, indicating that these MR-guided procedures are safe. Complication rates reported in the literature range between 0% and 3%, consistent with our study<sup>1,10,11</sup>.

In our study, the mean procedural time per lesion for MGWL and MGCB was 30 minutes and 45 minutes, respectively, similar to the literature<sup>9,10,11</sup>.

Previous studies have mentioned challenges in the application of MR-guided techniques, such as limited access to the lesion (e.g., those located near the skin, axillary tail, or chest wall or in the inner quadrants or retroareolar region of the breast), lesions with washout enhancement kinetics, marked breast parenchymal enhancement, and lesions in fatty breasts were mentioned in previously published articles<sup>3,5,16</sup>. All MR-guided biopsy procedures performed in our study resulted in technical success, as reported in the literature<sup>11,16</sup>.

The positive predictive value (PPV) of MR-guided biopsy procedures in this study was 24.5%, consistent with the values stated in previous studies in the literature<sup>2,10,12,17</sup>. Schneider et al. and Constance et al. found



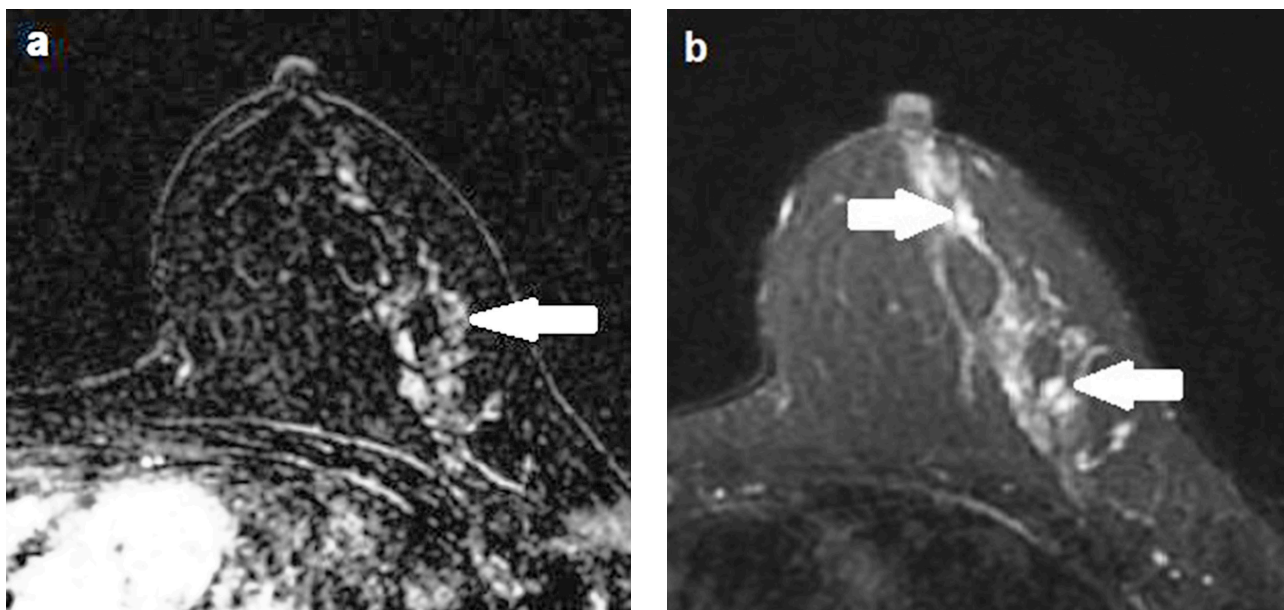


**Figure 4.** a–b. A 52-year-old woman with known familial high risk for breast cancer. Axial post-contrast T1-weighted fat-suppressed MR subtraction image shows non-mass enhancement with heterogeneous internal pattern and segmental distribution in the left breast (arrow) (a). Axial STIR MR image shows several millimeter-sized cystic lesions (arrows) in the non-mass enhancement area. After MR-guided needle localization and excisional biopsy, the pathological diagnosis was fibrocystic disease (b).

PPVs of 40%, which is considerably higher than in our study. These differences may be due to the low number of cases in their studies and the higher proportions of high-risk patients and patients with diagnosed breast cancer in the study populations compared to ours<sup>15,18</sup>. In our research, malignancy detection rates were similar for MGWL/excisional biopsy (23.9%) and MR-guided core biopsy (27.3%). In the study by Taneja et al., both biopsy techniques were used. Still, we could not find any data in the literature comparing the PPVs of the procedures<sup>11</sup>. However, the individual PPV values of both methods were consistent with those in the literature<sup>8,19</sup>.

As expected, we found a higher PPV (41.7%) in patients who underwent MR-guided biopsy to investigate the extent of cancer as compared to other indications. This rate was similar to some studies in the literature. It showed that preoperative breast MRI is an essential guide in the treatment management of patients with breast cancer<sup>9,10,20</sup>.

Of the malignant lesions in our study, 57.7% were diagnosed as ductal carcinoma in situ (DCIS), 13.8% as invasive ductal carcinoma, and 7.2% as invasive lobular carcinoma. In the studies by Morris et al. and Meucci et al., DCIS rates were 54.5% and 61.5%, respectively, and were higher than for invasive carcinoma, similar to our study<sup>7,10</sup>. As mentioned in the literature, clinically,

US-and MG-occult breast cancers are primarily early stage and can be visualized on MRI<sup>6,10,21,22</sup>. Therefore, we attribute the higher rate of DCIS to our study sample, which is comprised exclusively of MRI-only lesions<sup>10</sup>.

As stated in the literature, sclerosing adenosis can mimic malignancy by showing suspicious features on breast MRI more often than fibroadenoma and fibrocystic disease<sup>23,24</sup>. Therefore, in our study, including BI-RADS-MRI 4 and 5 lesions, the most common pathological diagnosis of benign lesions was sclerosing adenosis, which was an expected result.

The patient group selected for our study had MRI-only lesions for which an MR-guided biopsy was recommended. Little data in the literature regarding the diagnostic value of MRI findings in this patient group<sup>9,12</sup>. Many studies have shown that breast cancer most commonly occurs in the upper outer quadrant of the breast<sup>25</sup>. Surprisingly, we found approximately 6-fold higher odds of detecting a malignant lesion in the lower inner quadrant than in the upper outer quadrant. We believe the reason for this is that the MRI indication for the majority (55.5%) of patients with lower inner quadrant lesions was to evaluate the extent of breast cancer. However, Gao et al. found no relationship between lesion localization and malignancy<sup>9</sup>.

MR-guided biopsy was recommended for all lesions included in this study due to MRI findings suspicious of malignancy. This could explain the absence of a significant difference in predicting malignancy when comparing the morphological features and enhancement patterns of the lesions between the groups. Dratwa et al. found that NME lesions were more benign, while mass lesions with irregular shapes and margins were more malignant<sup>17</sup>. However, unlike our study, BI-RADS category 3 lesions were also included in their research, which may explain the discrepancy between our results.

According to the results of our study, the kinetic curve and BI-RADS classification of the lesions were significant predictors of malignancy (Table 3). As expected, lesions in our study that showed enhancement with a washout kinetic curve were significantly more likely to be cancer than those with a persistent or plateau kinetic curve. Previous studies in the literature have obtained similar results<sup>5,9,17</sup>.

Our study demonstrated that BI-RADS 5 lesions on MRI were more likely to be malignant than BI-RADS 4 lesions. This finding is similar to some studies in the literature<sup>17</sup>. Only one lesion that we classified as BI-RADS 5 was pathologically diagnosed as fibrocystic breast disease (Fig. 4). This lesion was segmental NME with a washout kinetic curve and heterogeneous internal enhancement. The patient was in the high-risk group for breast cancer. In the literature, the segmental distribution pattern of NME has been reported to have a significantly higher predictive rate for malignancy in the literature<sup>26,29</sup>. However, Morakkabati-Spitz et al. reported in their study that fibrocystic breast disease could present as segmental NME, as in our case<sup>30</sup>.

As observed in the study by Dratwa et al., lesion size, BD, and BPE were not found to contribute to the prediction of malignancy<sup>17</sup>.

Our study has several limitations. First, it is limited to a single-center experience with MGWL and MGCB. As a retrospective study, the sample size was small. Moreover, there was no comparative evaluation of the effects of MGWL and MGCB on cancer diagnosis and treatment management. Further studies may be designed to compare MGWL and MGCB in this

regard. Thirdly, given that only patients who underwent MR-guided biopsy procedures were included in the study, the findings do not represent all the lesions for which MR-guided biopsy was recommended. Finally, we did not refer to diffusion-weighted imaging (DWI) sequences when evaluating the lesions in our study. Apparent diffusion coefficients obtained from DWI images could also help predict the malignancy of lesions.

## Conclusion

In MRI-only lesions recommended for MR-guided biopsy, the lesions' BI-RADS-MRI category and kinetic curve type may help predict malignancy before biopsy. Our results showed that having a washout kinetic curve of enhancement and being BI-RADS-MRI category 5 were significant predictors of malignancy in these lesions.

## Authors' Contributions

Conceptualization, methodology: ACB, HA; Formal analysis and investigation: ACB, HA, IEB; Writing—original draft preparation: ACB, HA; Writing—review and editing: ACB, IEB; Supervision: ACB, HA, IEB.

## Conflict of Interest

The authors declare that they have no conflict of interest.

## Information Consent

This retrospective study was approved by the local institutional review board (Registration number: 2022–08/130), which waived the need for informed consent.

## Ethical Statement

All procedures conducted in studies involving human participants adhered to the ethical standards set by the institutional and national research committee, following the 1964 Helsinki Declaration and its subsequent amendments or comparable ethical standards.

## Information Concerning Grants

This research was carried out without any funding support.

## References

1. Wang Y-T, Huang C-S, Lee H-T, Chang Y-C, Liu H-M. MRI-guided Needle Localization for Breast Lesions Occult in Mammograms and Ultrasound. *Chin J Radiol.* 2008;33:1-7.
2. Carlson JW, Birdwell RL, Gombos EC, Golshan M, Smith DN, Lester SC. MRI-directed, wire-localized breast excisions: incidence of malignancy and recommendations for pathologic evaluation. *Hum Pathol.* 2007;38(12):1754-9.
3. van den Bosch MA, Daniel BL, Pal S, Nowels KW, Birdwell RL, Jeffrey SS, Ikeda DM. MRI-guided needle localization of suspicious breast lesions: results of a freehand technique. *Eur Radiol.* 2006;16(8):1811-7.
4. Floery D, Helbich TH. MRI-Guided percutaneous biopsy of breast lesions: materials, techniques, success rates, and management in patients with suspected radiologic-pathologic mismatch. *Magn Reson Imaging Clin N Am.* 2006;14(3):411-25.
5. Causer PA, Piron CA, Jong RA, Curpen BN, Luginbuhl CA, Glazier JE, et al. MR imaging-guided breast localization system with medial or lateral access. *Radiology.* 2006;240(2):369-79.
6. Olson JA Jr, Morris EA, Van Zee KJ, Linehan DC, Borgen PI. Magnetic resonance imaging facilitates breast conservation for occult breast cancer. *Ann Surg Oncol.* 2000;7(6):411-5.
7. Meucci R, Pistolesse Chiara A, Perretta T, Vanni G, Portarena I, Manenti G, et al. MR imaging-guided vacuum assisted breast biopsy: Radiological-pathological correlation and underestimation rate in pre-surgical assessment. *Eur J Radiol Open.* 2020;7:100244.
8. Eby PR, Lehman C. MRI-guided breast interventions. *Semin Ultrasound CT MR.* 2006;27(4):339-50.
9. Gao Y, Bagadiya NR, Jardon ML, Heller SL, Melsaether AN, Toth HB, et al. Outcomes of Preoperative MRI-Guided Needle Localization of Nonpalpable Mammographically Occult Breast Lesions. *AJR Am J Roentgenol.* 2016;207(3):676-84.
10. Morris EA, Liberman L, Dershaw DD, Kaplan JB, LaTrenta LR, Abramson AF, et al. Preoperative MR imaging-guided needle localization of breast lesions. *AJR Am J Roentgenol.* 2002;178(5):1211-20.
11. Taneja S, Jena A, Kumar K, Mehta A. Technical Note: MRI-guided breast biopsy - our preliminary experience. *Indian J Radiol Imaging.* 2010;20(3):218-20.
12. Spick C, Pinker-Domenig K, Rudas M, Helbich TH, Baltzer PA. MRI-only lesions: application of diffusion-weighted imaging obviates unnecessary MR-guided breast biopsies. *Eur Radiol.* 2014;24(6):1204-10.
13. Morris EA, Comstock CE, Lee CH. ACR BI-RADS® Magnetic resonance imaging. In: *ACR BI-RADS® Atlas, Breast imaging reporting and data system.* Reston, VA. American College of Radiology, 2013:56-71.
14. Rao AA, Feneis J, Lalonde C, Ojeda-Fournier H. A pictorial review of changes in the BI-RADS fifth edition. *Radiographics.* 2016;36(3):623-39.
15. Schneider JP, Schulz T, Horn LC, Leinung S, Schmidt F, Kahn T. MR-guided percutaneous core biopsy of small breast lesions: first experience with a vertically open 0.5T scanner. *J Magn Reson Imaging.* 2002;15(4):374-85.
16. Eby PR, Lehman CD. Magnetic resonance imaging-guided breast interventions. *Top Magn Reson Imaging.* 2008;19(3):151-62.
17. Dratwa C, Jalaguier-Coudray A, Thomassin-Piana J, Gonin J, Chopier J, Antoine M, et al. Breast MR biopsy: Pathological and radiological correlation. *Eur Radiol.* 2016;26(8):2510-9.
18. Lehman CD, Deperi ER, Peacock S, McDonough MD, Demartini WB, Shook J. Clinical experience with MRI-guided vacuum-assisted breast biopsy. *AJR Am J Roentgenol.* 2005;184(6):1782-7.
19. Peters NH, Meeuwis C, Bakker CJ, Mali WP, Fernandez-Gallardo AM, van Hillegersberg R, et al. Feasibility of MRI-guided large-core-needle biopsy of suspicious breast lesions at 3 T. *Eur Radiol.* 2009;19(7):1639-44.
20. Yi A, Cho N, Yang KS, Han W, Noh DY, Moon WK. Breast Cancer Recurrence in Patients with Newly Diagnosed Breast Cancer without and with Preoperative MR Imaging: A Matched Cohort Study. *Radiology.* 2015;276(3):695-705.
21. Orel SG, Schnall MD. MR imaging of the breast for the detection, diagnosis, and staging of breast cancer. *Radiology.* 2001;220(1):13-30.
22. Alaref A, Hassan A, Sharma Kandel R, Mishra R, Gautam J, Jahan N. Magnetic Resonance Imaging Features in Different Types of Invasive Breast Cancer: A Systematic Review of the Literature. *Cureus.* 2021;13(3):e13854.
23. Gity M, Arabkheradmand A, Taheri E, Shakiba M, Khademi Y, Bijan B, et al. Magnetic Resonance Imaging Features of Adenosis in the Breast. *J Breast Cancer.* 2015;18(2):187-94.
24. Guirguis MS, Adrada B, Santiago L, Candelaria R, Arribas E. Mimickers of breast malignancy: imaging findings, pathologic concordance and clinical management. *Insights Imaging.* 2021;12(1):53.
25. Chan S, Chen JH, Li S, Chang R, Yeh DC, Chang RF, et al. Evaluation of the association between quantitative mammographic density and breast cancer occurred in different quadrants. *BMC Cancer.* 2017;17(1):274.
26. Tozaki M, Fukuda K. High-spatial-resolution MRI of non-masslike breast lesions: interpretation model based on BI-RADS MRI descriptors. *AJR Am J Roentgenol.* 2006;187(2):330-7.
27. Lunkiewicz M, Forte S, Freiwald B, Singer G, Leo C, Kubik-Huch RA. Interobserver variability and likelihood of malignancy for fifth edition BI-RADS MRI descriptors in non-mass breast lesions. *Eur Radiol.* 2020;30(1):77-86.
28. Tozaki M, Igarashi T, Fukuda K. Breast MRI using the VIBE sequence: clustered ring enhancement in the differential diagnosis of lesions showing non-masslike enhancement. *AJR Am J Roentgenol.* 2006;187(2):313-21.
29. Uematsu T, Kasami M. High-spatial-resolution 3-T breast MRI of nonmasslike enhancement lesions: an analysis of their features as significant predictors of malignancy. *AJR Am J Roentgenol.* 2012;198(5):1223-30.
30. Morakkabati-Spitz N, Leutner C, Schild H, Traeber F, Kuhl C. Diagnostic usefulness of segmental and linear enhancement in dynamic breast MRI. *Eur Radiol.* 2005;15(9):2010-7.